

Electronic Supporting Information for

Fabrication of silver nanoparticles with limited size distribution on TiO₂ containing zeolites

Andrea Mazzocut,^a Eduardo Coutino-Gonzalez,^b Wouter Baekelant,^b Bert Sels,^c Johan Hofkens,^{a,b} and Tom Vosch^{a,*}

^aNano-Science Center, Department of Chemistry, University of Copenhagen, Universitetsparken 5, 2100 Copenhagen, Denmark.

^bDepartment of Chemistry, KULeuven, Celestijnenlaan 200F, B-3001 Leuven, Belgium

^cDepartment of Microbial and Molecular Systems, Centre for Surface Chemistry and Catalysis, KULeuven, Kasteelpark Arenberg 23, B-3001 Leuven, Belgium

*Corresponding author: Tom Vosch, tom@chem.ku.dk

S1. Scanning electron microscope (SEM) pictures and chemical composition of LTA (3A, 4A, 5A) and FAU (Y) zeolites used in this study.

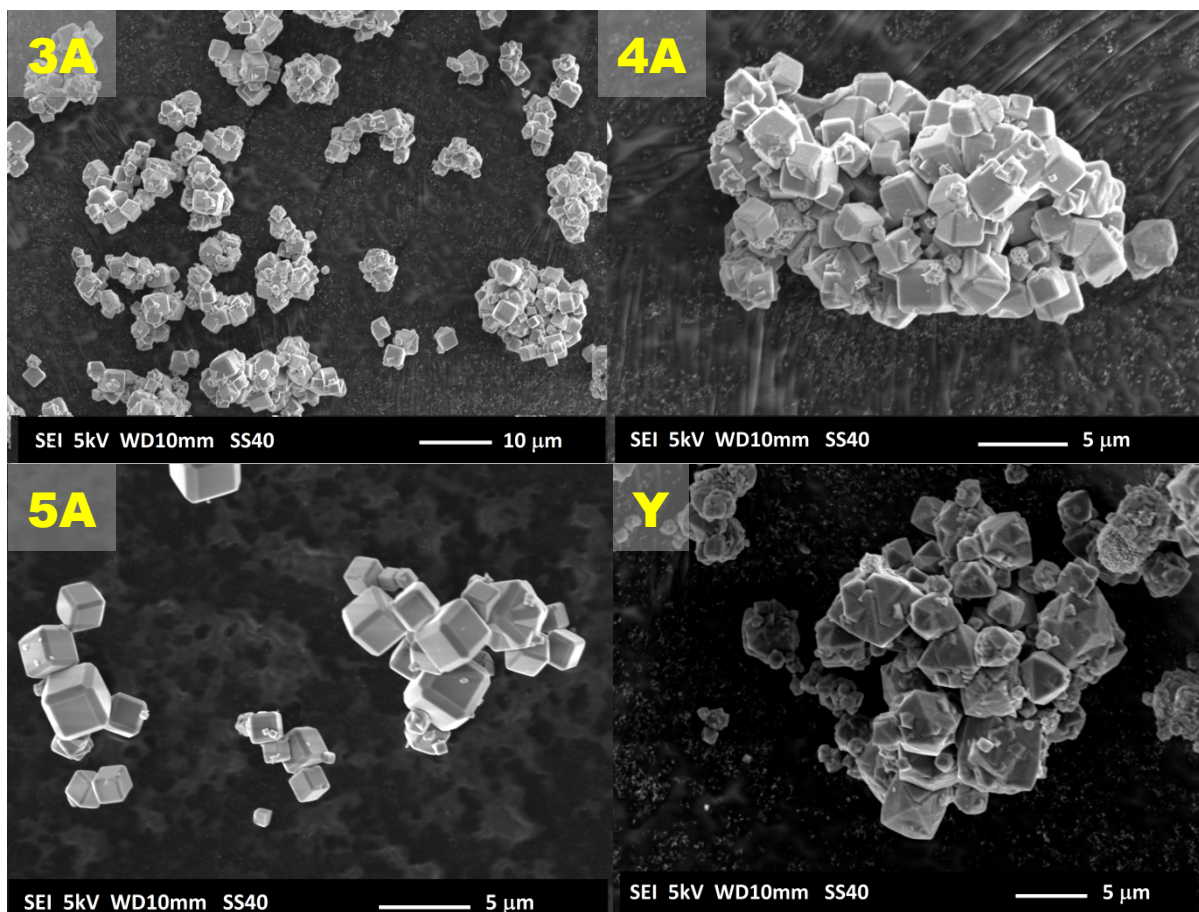


Figure S1. SEM images of the starting materials used in this study, 3A, 4A, 5A and Y zeolites. The images were recorded using a JEOL-6010LV SEM (non-coated samples). LTA topology (3A, 4A and 5A) presents a truncated cubic structure whereas FAU (Y) zeolites has a typical octahedral shape.

In Table S1 the chemical composition of the four zeolites employed in this study is shown. They have different silicon to aluminium ratios (Si/Al). LTA (3A, 4A and 5A) possess Si/Al ratios of 1 whereas FAU (Y) has a Si/Al of 2.7.

Table S1. Chemical composition of a unit cell of the different zeolites used in this study.

Zeolite	Structural formula
3A	$ \text{K}^+_{12} [\text{Al}_{12}\text{Si}_{12}\text{O}_{48}] \text{H}_2\text{O} _{27}$
4A	$ \text{Na}^+_{12} [\text{Al}_{12}\text{Si}_{12}\text{O}_{48}] \text{H}_2\text{O} _{27}$
5A	$ \text{Ca}^{2+}_6 [\text{Al}_{12}\text{Si}_{12}\text{O}_{48}] \text{H}_2\text{O} _{27}$
Y	$ \text{Na}^+_{6.5} [\text{Al}_{6.5}\text{Si}_{17.5}\text{O}_{48}] \text{H}_2\text{O} _{27.5}$

The structural formulas were obtained after normalization of the total amount of T atoms in the unit cell to 24.

S2. Artificial UV irradiation set-up description.

The samples used in Figure 4 and Figure 5 in the main text were irradiated using an in-house circular photo-reactor containing 12 vertical UV lamps (366 nm), the typical emission spectrum of the 366 nm lamp is displayed in Figure S2. The power was regulated by the amount of lamps used. The samples were exposed for 15 minutes in the photoreactor to an intensity of about 1mW/cm².

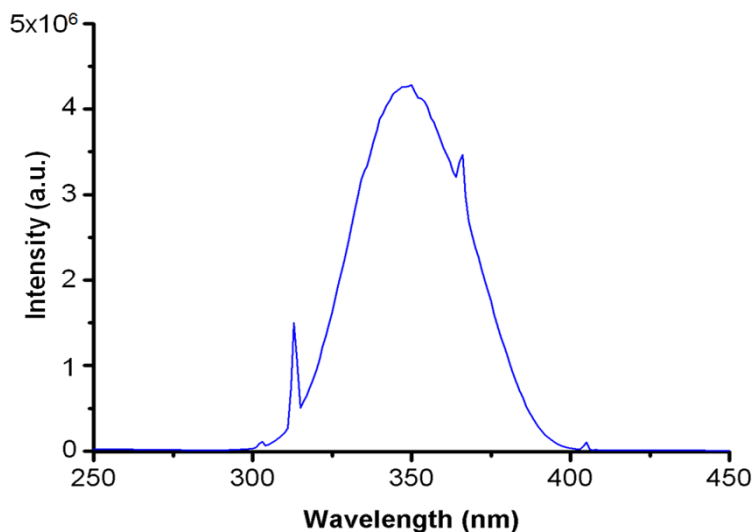


Figure S2. Typical emission spectrum of the 366 nm lamps employed in the UV reactor. The samples exposed to 15 minutes UV irradiation in Figure S11 and S12 were irradiated with a handheld 366 nm UV lamp.

Table S2. Pore diameter size of the zeolite materials employed in this study and silver nanoparticle size distribution.

Sample	Pore diameter¹ (nm)	Average Ag NP size (nm)	Fit dispersion FWHM (nm)	Irradiation conditions
3A_8Ag10Ti	0.3	4.5	3	Sunlight 2 days
4A_8Ag10Ti	0.4	6.5	3	Sunlight 2 days
5A_8Ag10Ti	0.5	5	2.5	Sunlight 2 days
Y_8Ag10Ti	0.7	9.5	8.5	Sunlight 2 days
5A_8Ag10Ti	0.5	20	30	Handheld UV lamp 15 min

The silver particle dimension on the zeolites surface are larger than the openings and cavities found in the zeolite material (Table S2), indicating that smaller silver species diffuse through the openings to form large nanoparticles on the surface. Nevertheless, a small difference in silver particle size distribution was found between the sunlight exposed Ag/Ti containing zeolite A and Y, a wider range of size distributions was observed in Y_8Ag10Ti. The slightly larger cavities encounter in Y zeolite with respect to zeolite A (3A, 4A, 5A) might be the cause of such difference.

S3. XRD analysis of the parent zeolites, silver exchanged and photo-reduced Ti impregnated and sol-gel encapsulated zeolites.

XRD was used to investigate the degree of functionalization of the materials as well as to monitor the change in the crystallinity of the material. The samples were mounted in a Stoe Stadi-P powder diffractometer and the data were collected with 2 theta angle from 2 to 50° using a Cu K-Alpha (1.54 Å) radiation source.

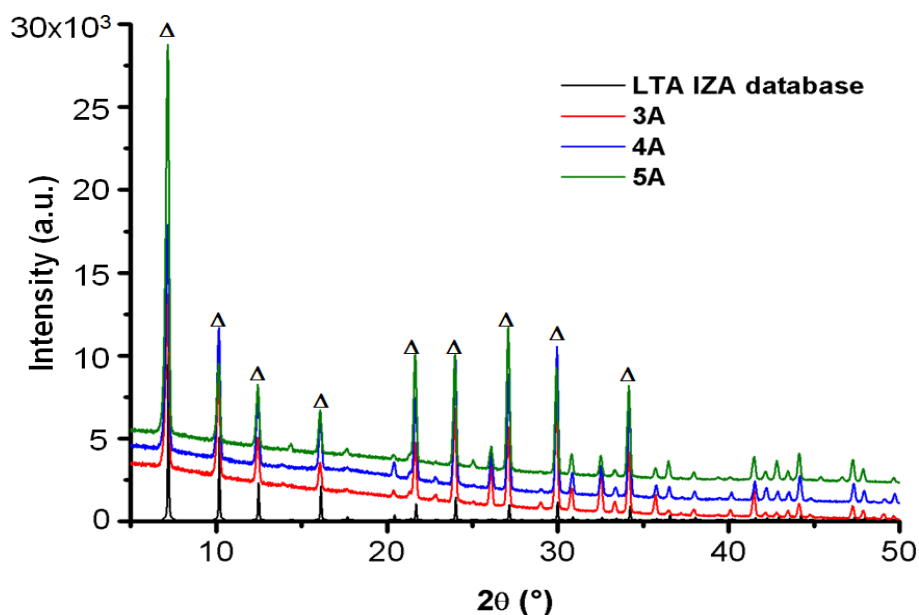


Figure S3. Powder diffraction pattern for LTA zeolites showing the LTA IZA reference¹ and the commercial samples used in this study. The typical zeolite LTA XRD peaks are indicated with Δ .

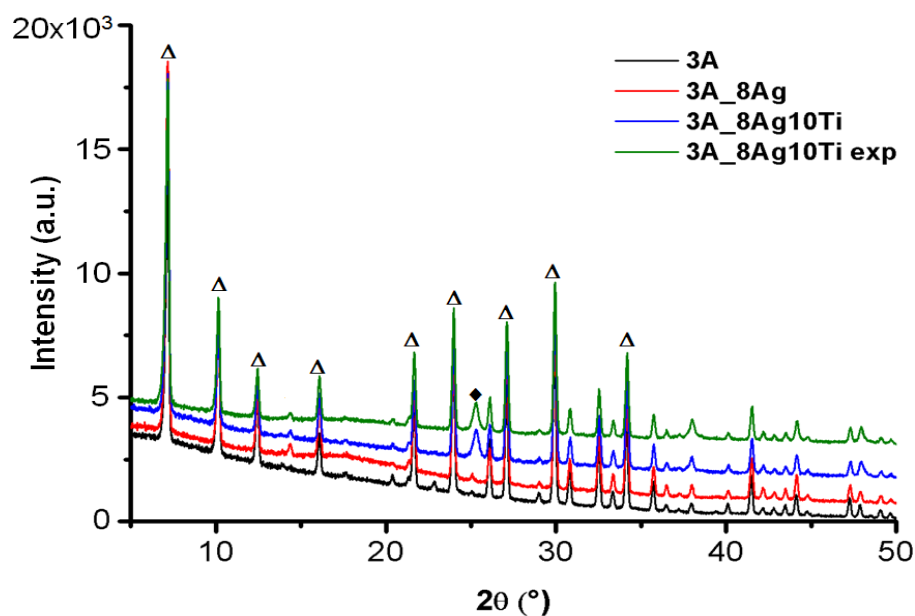


Figure S4. Powder diffraction pattern for 3A zeolites. The blank sample was compared to the silver exchanged and the Ag/Ti containing zeolites before and after the photo-reduction. Zeolite LTA XRD patterns are indicated with Δ , whereas \blacklozenge was used to indicate the positions of the reflection peaks due to TiO_2 in its anatase phase.

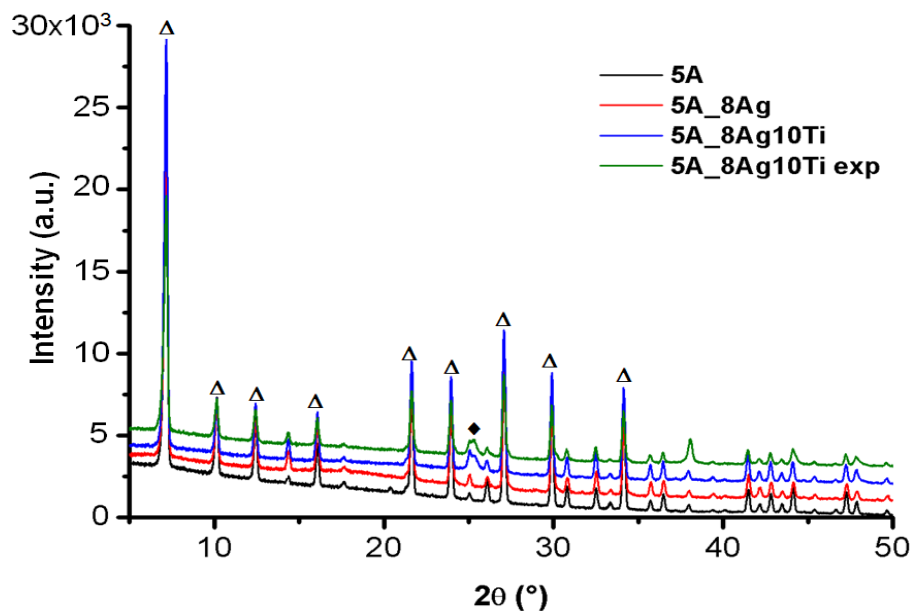


Figure S5. Powder diffraction pattern for 5A zeolites. The blank sample was compared to the silver exchanged and the Ag/Ti containing zeolites before and after the photo-reduction. For the explanation of the symbols *vide supra*.

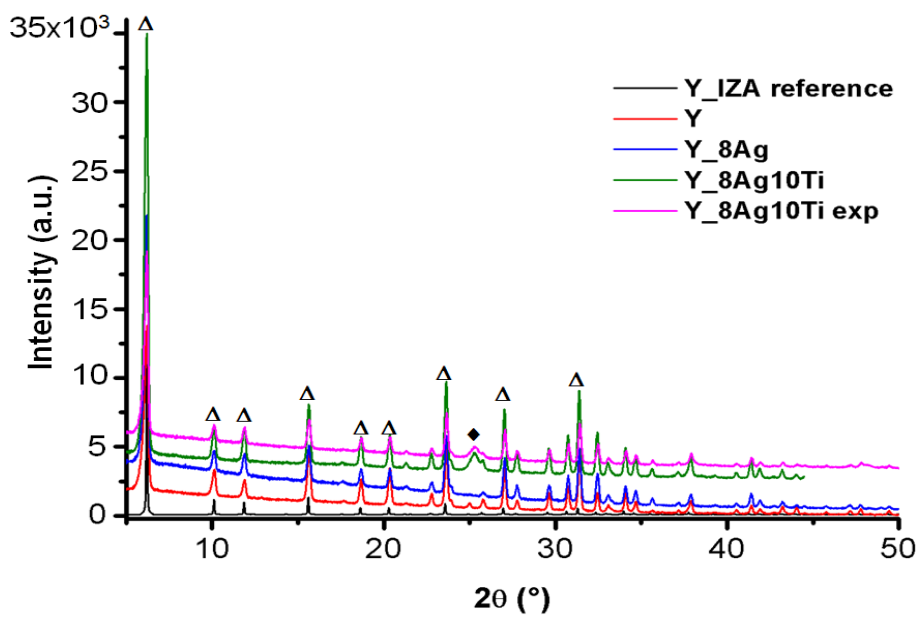


Figure S6. Powder diffraction pattern for Y zeolites. The blank sample was compared to the silver exchanged and the Ag/Ti containing zeolites before and after the photo-reduction. For the explanation of the symbols *vide supra*.

S4. Single crystal fluorescence microscopy and steady-state spectrofluorimetry.

A wide-field fluorescence microscope (Olympus IX71) coupled to a UV/Vis lamp (X-Cite Series 120Q) was used to monitor the change in fluorescence signal due to the photo-reduction of silver cluster at the single crystal level. All the samples were investigated under UV illumination using the Olympus U-MWU2 fluorescence mirror unit (wavelength 330-385 nm, output power 23 mW) with a 40X, 0.6 NA Olympus objective. The pictures were recorded with a RGB camera (Thorlabs DCC1645C) mounted on the microscope.

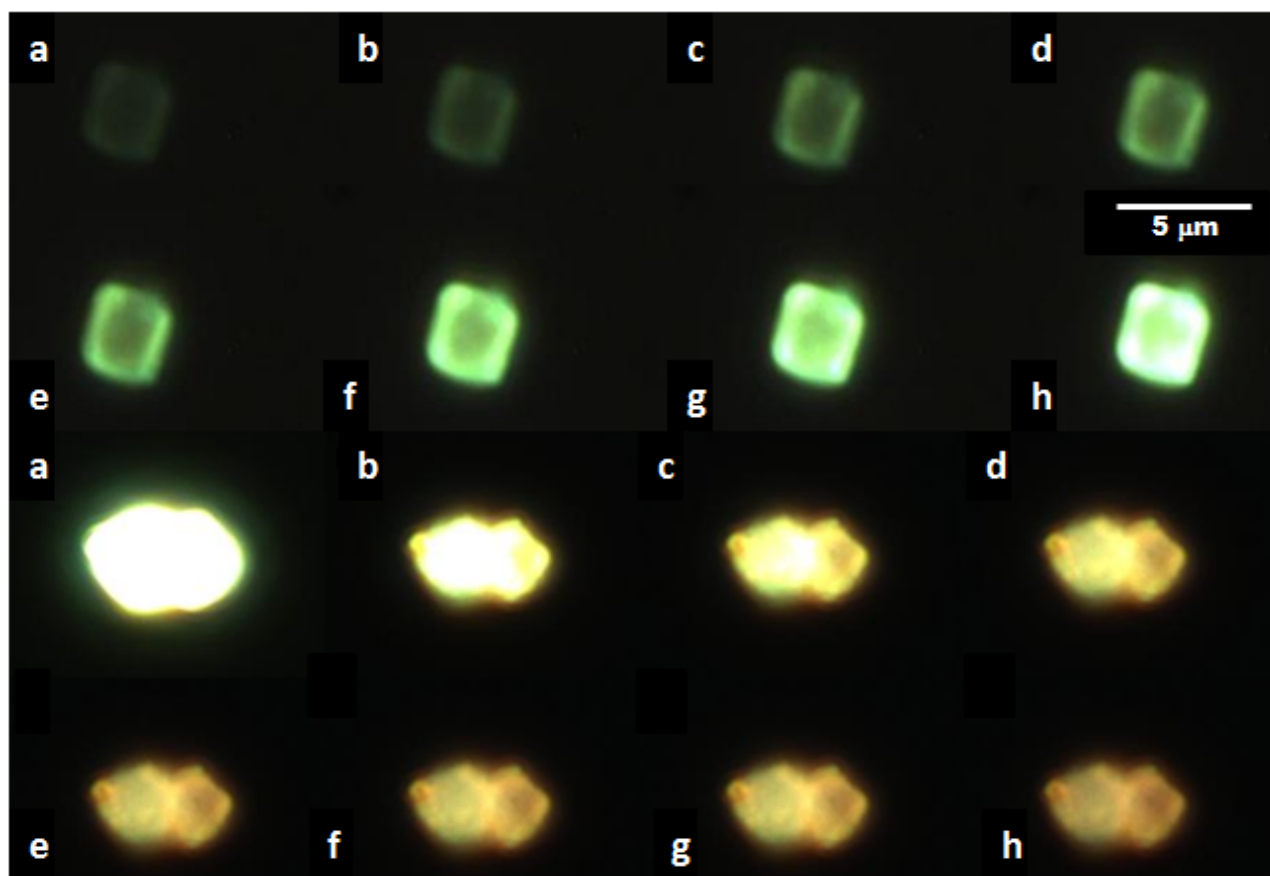


Figure S7. True color fluorescence microscopy images of 3A_8Ag (top panel) and day light-exposed 3A_8Ag10Ti (bottom panel) upon UV excitation. Time interval between images, 10 seconds. The clearly visible photoactivation of the luminescent silver clusters in 3A_8Ag was replaced by a fast photobleaching of the luminescence in 3A_8Ag10Ti.

For the emission-excitation characterization at bulk level, the samples were placed in a quartz cuvette (1 mm path length). Emission and excitation spectra were recorded using an Edinburgh Instruments FLS 980 fluorimeter coupled to an integrating sphere (Labsphere). For every excitation wavelength, the emission was collected starting 10 nm above the excitation wavelength and ending at 800 nm using 10 nm steps. The signal above 410 nm was measured using a 400 nm long pass glass filter to avoid interference from second-order excitation peaks, the measured intensities were corrected for the transmittance of the long pass filter. The emission was collected in “front face mode” and send to a PMT for detection. From the separate emission spectra at varying excitation wavelengths, the two dimensional excitation-emission matrices were constructed; the raw data was corrected for background and noise and interpolated to a resolution of 1 nm x 1 nm. All the scans were recorded using the same settings (integration time 0.1 s, integration step 1nm, excitation slit 10 nm, emission slit 6 nm). The use of an integrating sphere and the same measurement settings allowed us to perform the analysis of the loss of emission in the samples after UV exposure in a quantitative way.

The loss of luminescence after UV exposure in the samples was monitored by recording two-dimensional (2D) excitation emission scans and comparing the emission profiles with respect to the illumination time. The samples were left for 5, 10, and 15 minutes in the photoreactor (366 nm, 1mW/cm²), then were transferred to a quartz cuvette and measured using the above described set-up. In Figure S8-A the 2D plot of 3A_8Ag10Ti non-illuminated is presented, a characteristic green emission (maximum around 540 nm) was observed when the sample was excited at 390 nm. The same emission profile was found in the UV irradiated 3A_8Ag10Ti samples, however a decrease in the emission intensity was observed. This is clearly represent in Figure S8-B for 3A_8Ag10Ti UV

irradiated samples, after 15 minutes of UV illumination the emission intensity decreased by a factor of 4 compared to the non-irradiated sample.

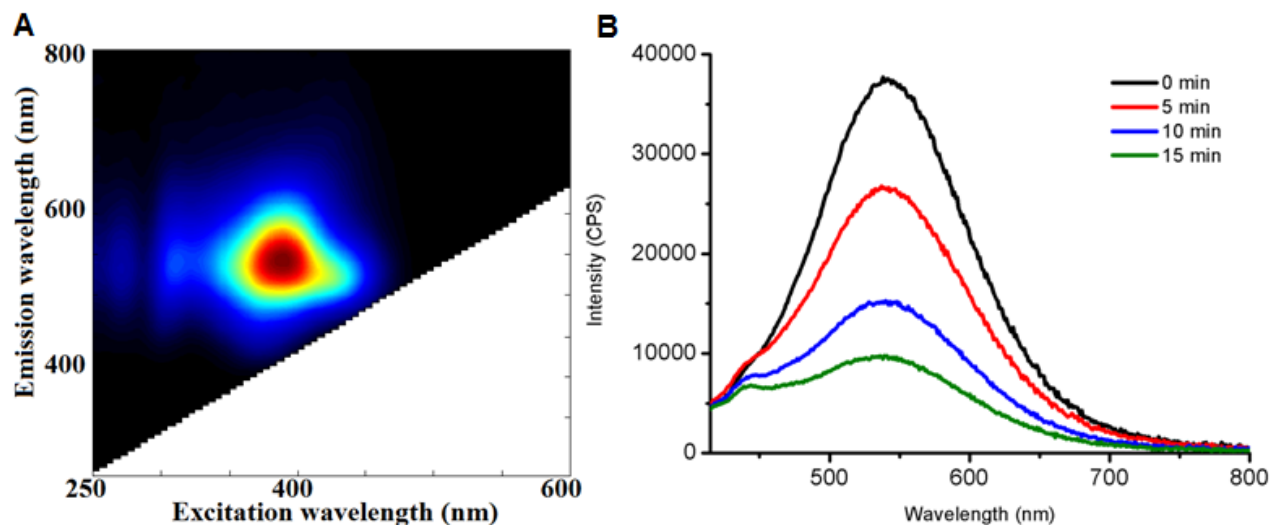


Figure S8. (A) Two-dimensional excitation-emission spectra of 3A_8Ag10Ti as prepared (non-UV illuminated), a green emission was observed in the samples with maximum at around 540 nm at 390 nm excitation wavelength. (B) Emission spectra of 3A_8Ag10Ti at different UV irradiation times (photoreactor), excitation wavelength 390 nm.

S5. Analysis of the samples using scanning & transmission electron microscopy (SEM, TEM) and energy-dispersive X-ray spectroscopy (EDX).

A JEOL-6010LV SEM microscope was employed to study the silver nanoparticles distribution on the surfaces of the zeolite crystals, the samples were deposited onto a carbon tape for visualization.

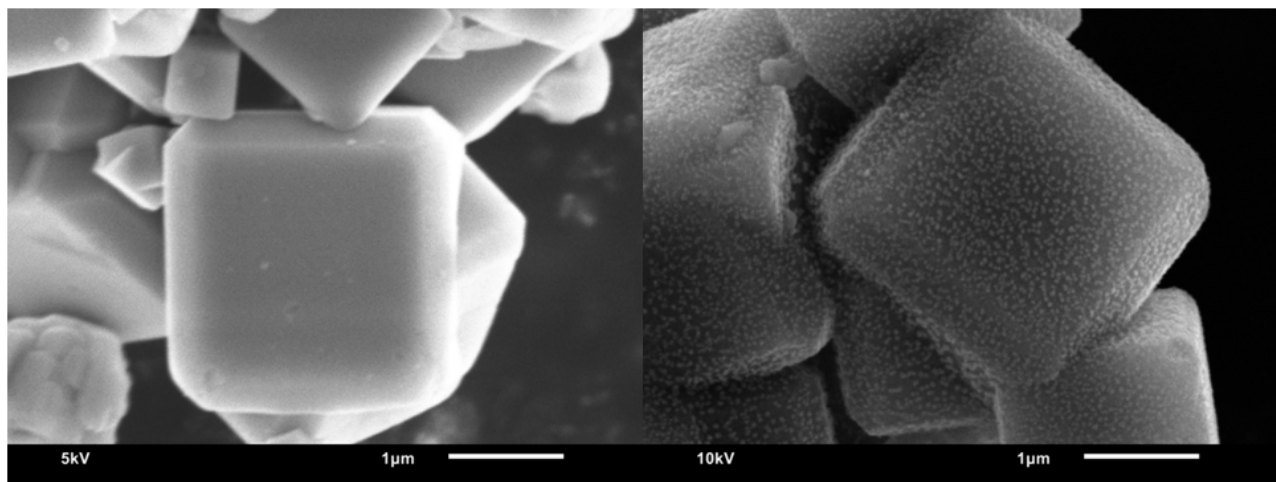


Figure S9. SEM images of non-illuminated (left) 4A_8Ag10Ti and (right) UV irradiated (15 minutes) 4A_8Ag10Ti.

A Philips CM20 TEM operating at 200 kV was used to investigate the particles and estimate their average particle size. A series of glass test-tubes were filled with a 1 mg/ml water suspension of silver-titanium zeolites and left for 2 days near the window, exposed to daylight. To obtain a uniform irradiation, the samples were occasionally shaken to avoid the powder deposition. A 5 μ L droplet of solution was placed on a TEM copper grid and left to evaporate. The same procedure was followed for the artificial irradiated samples, the main difference here was the irradiation source (366 nm UV lamp, 1mW).

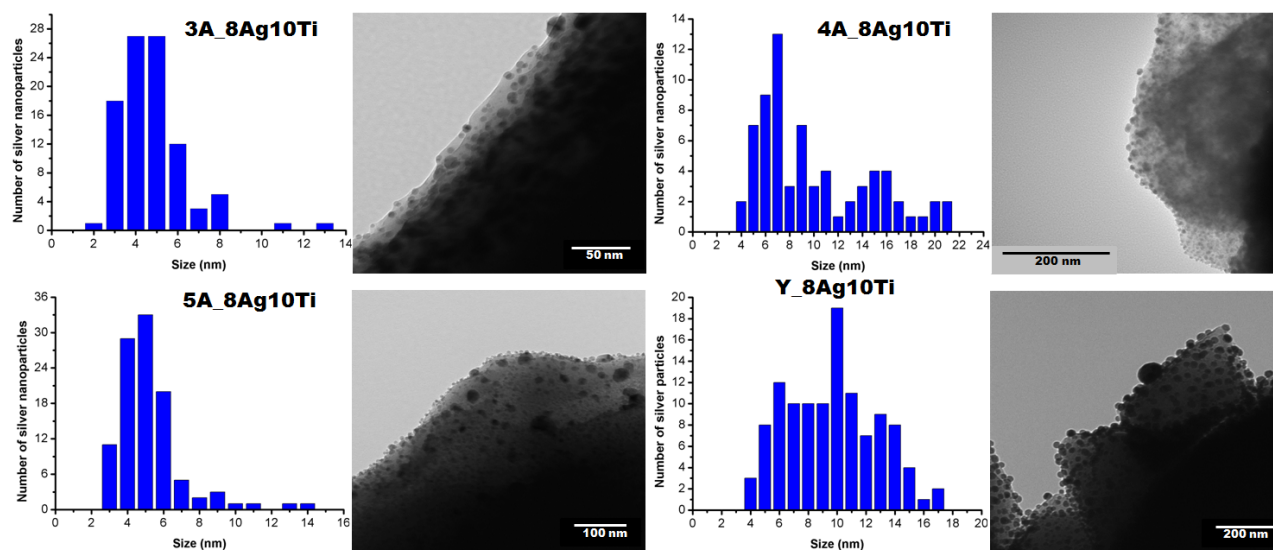


Figure S10. TEM images of daylight exposed 3A_8Ag10Ti, 4A8Ag10Ti, 5A_8Ag10Ti and Y_8Ag10Ti. The silver nanoparticle size distribution is also indicated.

The particles size was estimated on the basis of approximately one hundred measurements, in the same zeolite crystal, for each sample. These diameters were then plotted in an histogram, and fitted with a Gaussian distribution in which the maximum peaks were taken as the average aggregates diameters. The computed results, shown in Figure S10, for daylight irradiated 3A_8Ag10Ti, 4A8Ag10Ti, 5A_8Ag10Ti & Y_8Ag10Ti respectively, indicate a small but remarkable dependence of the silver nanoparticles dimensions with respect to the zeolite framework used (LTA and FAU).

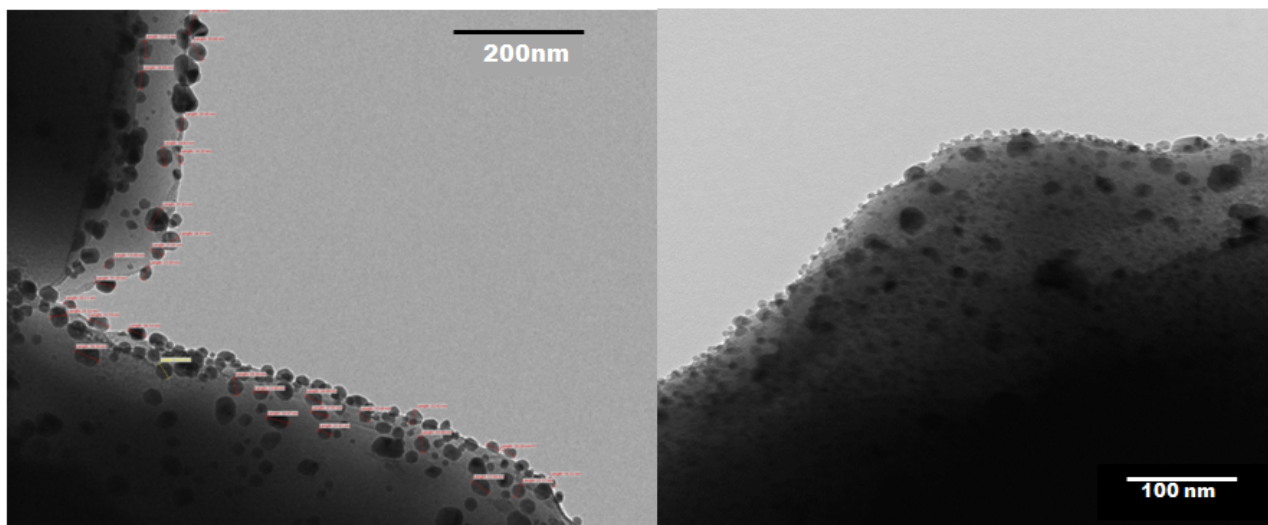


Figure S11. TEM micrograph of 5A_8Ag10Ti zeolite irradiated with a handheld UV lamp (366 nm, 1mW), for 15 minutes (left), and daylight exposed (right). The more intense energy of the UV lamp led to the formation of bigger and less well defined silver nanoparticles.

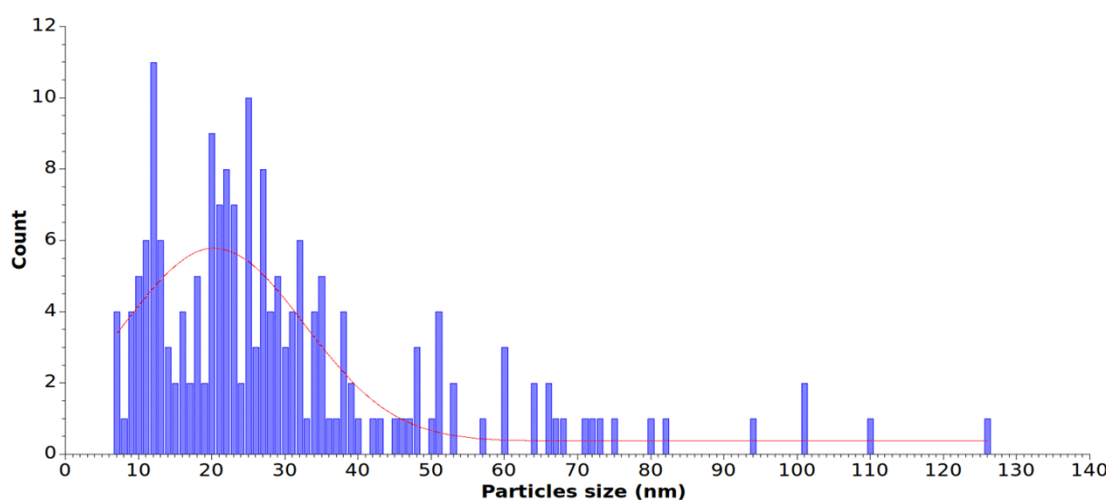


Figure S12. Particle size distribution for 5A_8Ag10Ti exposed to a UV lamp ($\lambda=366$ nm, output power 1 mW) for 15 minutes.

In the samples exposed to an artificial irradiation (UV handheld lamp, 366 nm) the particle size distribution was found larger compared to the natural irradiated samples (daylight), an average particle size of about 20 nm was observed (Figure S11 & S12).

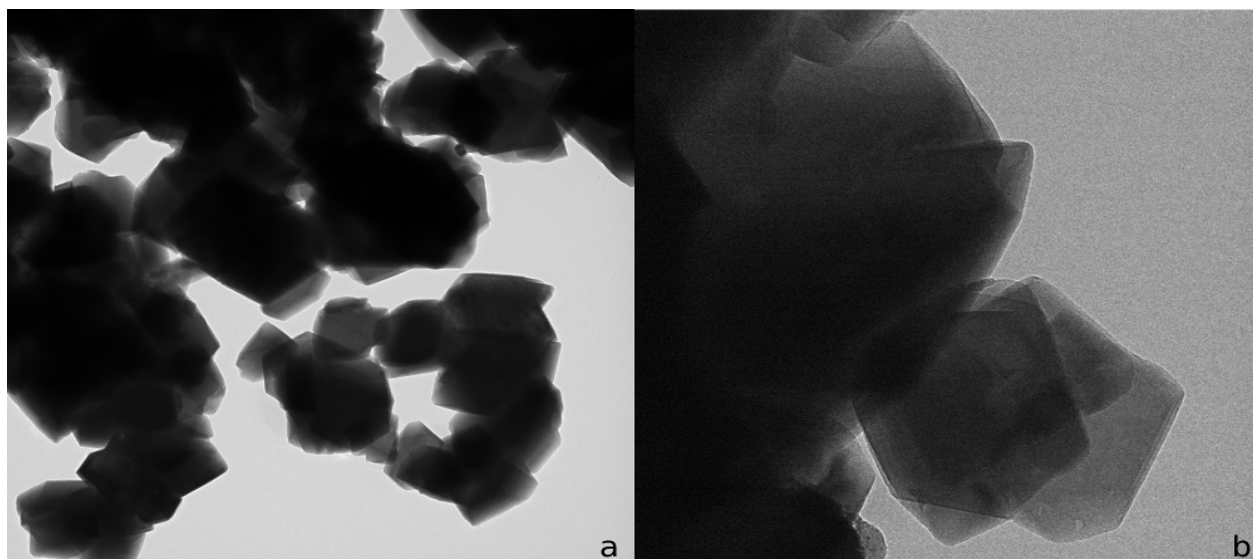


Figure S13. TEM micrographs of Ag-free Y₁₀Ti zeolites exposed to UV. The presence of only TiO₂ did not lead to the formation of nanoparticles on the surface of the zeolite crystals.

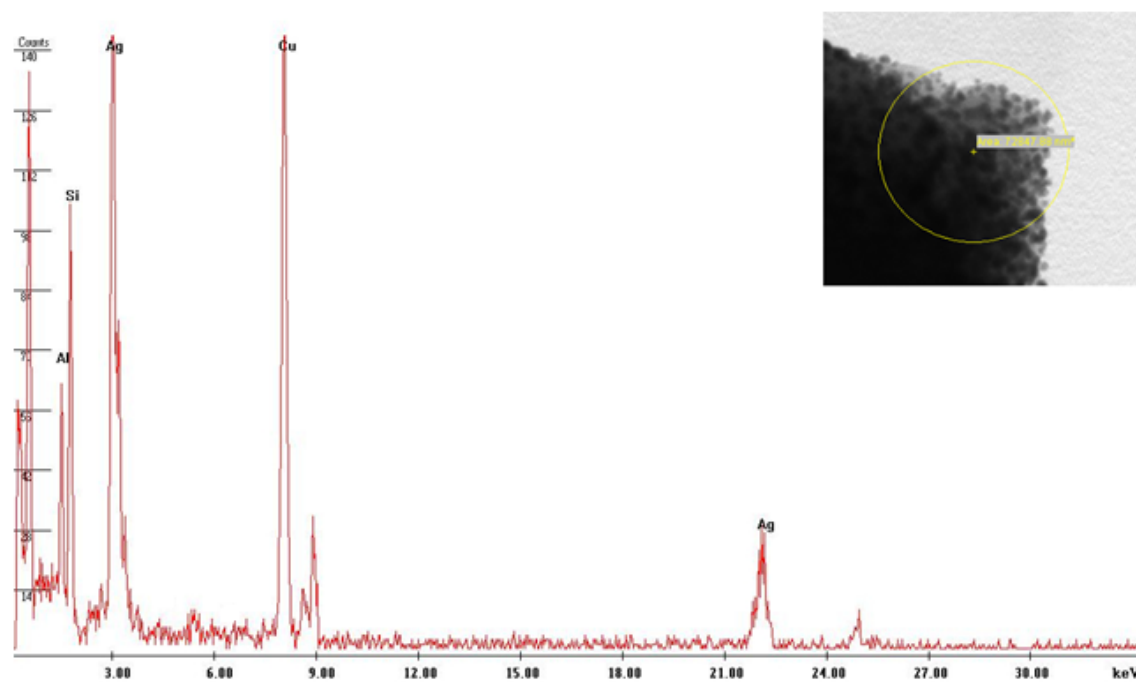


Figure S14. EDX analysis of daylight exposed Y₈Ag₁₀Ti zeolite. The presence of silver is observed. An area of approximately 270 x 270 nm was examined in each sample.

References

- (1) International Zeolite Association. <http://www.iza-online.org>.